

Ultracold Metastable Helium: from Atoms to Exotic Molecules¹

Michèle Leduc* and Claude Cohen-Tannoudji

Collège de France and Laboratoire Kastler Brossel,[†]
Département de Physique de l'École Normale Supérieure 24 rue Lhomond F-75231 Paris Cedex 05, France

*e-mail: michele.leduc@physique.ens.fr

Received February 16, 2009

Abstract—We have written this article in the honor of our friend Vladilen Lethokov, who has produced so many brilliant ideas and results in the field of atomic and molecular physics and with whom we have had frequent unlightening discussions. We hope that the work described here will contribute to illustrate the richness of the field.

DOI: 10.1134/S1054660X09170101

1. INTRODUCTION

The helium atom is one of the simplest existing atoms. The wave functions of this two electron system are relatively well known. This makes it an appealing candidate for all sorts of high precision measurements and checks of theoretical predictions in atomic physics as well as in quantum chemistry. The most abundant isotope, present in the air, is ⁴He; it carries no nuclear spin and has no hyperfine structure, which is a factor of simplicity. Spectroscopic measurements of high accuracy, making use of optical pumping and magnetic resonance, have been performed in the ground state and the excited states of this atom, providing for instance a value of the fine structure constant and several tests of Quantum Electrodynamics. On the other hand, the odd isotope ³He carries a 1/2 nuclear spin, which makes it a rich playground in many domains of physics.

Actually the 1^1S_0 ground state of the helium atom is very difficult to manipulate with light, as the optical transition connecting it to the excited atomic states fall deep in the UV. The first excited state is the triplet metastable state 2^3S_1 , which is very long lived (8000 s) and carries a very large electronic energy of 20 eV. It can be considered as a sort of ground state under many circumstances. It is easily manipulated by light using the atomic $2^3S_1-2^3P$ transitions (see Fig. 1) for which convenient solid state lasers have been developed over the last three decades. Our teams at ENS have used this possibility for many different sorts of experiments involving either the ³He or the ⁴He isotopes.

We were initially interested in developing methods to magnetize gas samples of the ³He isotope: the 2^3S_1 metastable state is polarized by laser optical pumping and its polarization is transferred to the 1^1S_0 ground

state by metastability exchange collisions [1]. This provided polarized targets for nuclear physics and for neutron spin filters [2], as well as samples of hyperpolarized gas for lung imaging by magnetic resonance. In the 1980s, we were primarily involved in the study of quantum effects with spin polarized ³He at low temperature, demonstrating the spectacular changes of the transport properties of the gas resulting from the spin magnetization, as a consequence of the Pauli symmetrization principle in quantum mechanics [3]. In particular the existence of spin waves in the ³He polarized gas was evidenced in an experiment run in the 1–4 K range [4], which now finds a recent echo in the physics of Bose–Einstein condensation at much lower temperature.

When laser cooling started to develop in many laboratories in the world and also at ENS, our teams were tempted to apply these methods to ⁴He. It was clear that the ground state could not be a candidate, as it cannot be easily manipulated by light. A breakthrough occurred when laser cooling could be successfully

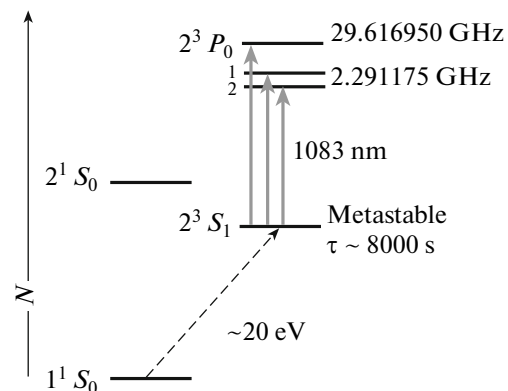
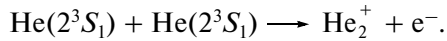


Fig. 1. A few energy levels of the helium atom.

¹ The article is published in the original.

[†] Unité de Recherche de l'École normale supérieure et de l'Université Pierre et Marie Curie, associée au CNRS.

applied to the ^4He atom in its 2^3S_1 metastable state, using the laser already developed for polarizing ^3He . However metastable atoms differ substantially from laser cooled alkali atoms in that they are very fragile: when two such atoms collide, they have a large probability to be destroyed by Penning ionization, resulting in the formation of ground state atoms, helium ions and electrons, according to the reactions:



Fortunately, as predicted by early articles of Gora Shlyapnikov, such collisions can be strongly inhibited when the electronic spins are polarized, because the total spin cannot be carried out by the collision products [5]. We took advantage of this property to reach Bose–Einstein condensation of metastable helium atoms.

This article will first recall the creation of a magneto-optical trap and then describe the method used to cool the gas much below the recoil limit by Velocity Selective Coherent Population Trapping (VSCPT). A very large increase in phase space density was then achieved by evaporation in a magnetic trap, taking advantage of the inhibition of the Penning collisions by the spin polarization, as mentioned above. We succeeded at observing the Bose–Einstein condensation of metastable helium in 2001 [6], simultaneously with the group of Alain Aspect in Orsay [7], a premiere for an atom in an excited state. In order to fully understand the dynamical properties of the condensate, a good knowledge of the s -wave scattering length a between two colliding metastable atoms is requested. Actually the value of a that we deduced from the expansion of the condensate was lacking precision, because of the uncertainty in the determination of the number of atoms in the sample. This is the reason why we then embarked in the study of helium molecules, with the idea to determine a through the position of the least bound molecular state in the interaction potential between two polarized metastable atoms.

This article will thus describe how ultracold molecules of helium were obtained by photoassociation of two metastable atoms. The physics of such exotic molecules, where two atoms are excited, happened to be very rich. It allowed one to produce dimmers of a giant size and to perform tests of fundamental problems such as the retardation effects in large size dimmers [8], as well as very accurate measurements of the energy and of the life time of bound states of these exotic molecules [9]. This article will in particular stress the analogies between methods used in VSCPT cooling for atoms and in atom-molecule dark resonances for two-photon photoassociation, in both cases based on the interference between transition probabilities in a Λ -type level scheme.

2. DARK STATE COOLING BELOW THE SINGLE PHOTON RECOIL LIMIT

2.1. Doppler Cooling with the $2^3S_1 \longleftrightarrow 2^3P_2$ Transition

Laser cooling of metastable helium is operated using laser light in the infrared tuned to the $2^3S_1 \longleftrightarrow 2^3P_2$ closed transition at 1083 nm. The saturation intensity for this transition is 0.16 mW/cm² and the linewidth 1.6 MHz. For a long time, the laser system was based on Ar-pumped solid state LNA lasers. They are now replaced by DBR laser diodes in an extended cavity configuration, injecting Yb doped fiber amplifiers delivering several Watts of continuous power. The emission is single mode with a typical linewidth of 300 kHz.

The preparation of the atomic sample begins with a beam of helium that is excited into the 2^3S_1 metastable state by a high voltage continuous discharge, cooled to liquid nitrogen temperature. A metastable helium beam emerges into an empty vacuum chamber. Radiation pressure on the metastable beam allows one to increase its collimation and to deflect it from the ground state helium beam. The metastable atoms are then decelerated in a Zeeman slower by a laser beam directed opposite to the atomic beam. Repeated absorption processes slow the atoms down from speeds nearly 1000 m/s to less than a 20 m/s over a distance of 2 m. The atoms are then collected in a magneto-optical trap (MOT) in a quartz cell sustaining a background pressure below 10^{-10} Torr, where in a few seconds up to 10^9 metastable atoms accumulate at a peak atomic density of 10^{10} cm⁻³.

In order to fully characterize the atomic cloud, we used an absorption method with a probe laser beam on resonance, which is turned on after the MOT field and light beams have been turned off. When the probe beam travels as a progressive wave, it gives the total absorption by the atoms from which the atomic density can be estimated. When it travels as a stationary wave, one can use a large laser intensity, typically $I \approx I_{\text{sat}}$, without displacing the atomic cloud. We thus can register spatially resolved images on a CCD camera with a good enough contrast, even if the detection efficiency of the camera is low at this wavelength.

The temperature of the gas is determined from the expansion of the cloud in free fall using the time of flight method. Images are taken a few milliseconds after the MOT laser beams are turned off. The temperatures obtained are on the order of 1 mK, close to the Doppler limit of the cooling.

2.2. Velocity Selective Coherent Population Trapping

It is possible to cool metastable helium atoms below the Doppler limit, and even below the single photon recoil limit, by using velocity selective dark resonances. Coherent population trapping, at the ori-

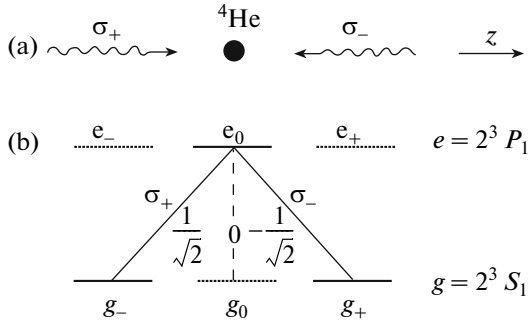


Fig. 2. (a) $\sigma_+ - \sigma_-$ laser configuration exciting the $2^3S_1 \leftrightarrow 2^3P_1$ transition of helium. (b) Pure three-level Λ configuration $\{g_-, e_0, g_+\}$ obtained after a few optical pumping cycles.

gin of dark resonances, can be achieved with Λ -type atomic systems. Such systems are realized for metastable helium atoms interacting with two counterpropagating σ_+ and σ_- polarized laser beams exciting the $2^3S_1 \leftrightarrow 2^3P_1$ transition (see Fig. 2 which represents the Zeeman sublevels and some useful Clebsch–Gordan coefficients for this transition). Since the $g_0 \leftrightarrow e_0$ transition is forbidden atoms are pumped in g_+ and g_- after a few fluorescence cycles. These two levels are coupled only to e_0 and a closed three level Λ configuration is realized (full lines of the figure).

Before presenting the dark state cooling of helium with the $2^3S_1 \leftrightarrow 2^3P_1$ transition, we briefly describe the properties of dark resonances and their physical interpretation. Consider a general three-level Λ -type configuration, with two lower levels g_1, g_2 , and one upper level e , excited by 2 laser waves $E_1 \exp[i(\mathbf{k}_1 \cdot \mathbf{r} - \omega_1 t)] + \text{c.c.}$ and $E_2 \exp[i(\mathbf{k}_2 \cdot \mathbf{r} - \omega_2 t)] + \text{c.c.}$ exciting the 2 transitions $g_1 \rightarrow e$ and $g_2 \rightarrow e$, respectively (see Fig. 3a). Let Δ be the detuning from Raman resonance:

$$\hbar\Delta = \hbar\omega_1 - \hbar\omega_2 - (E_{g_2} - E_{g_1}). \quad (1)$$

This detuning Δ can be varied by varying the splitting between g_1 and g_2 , ω_1 and ω_2 being fixed, or by sweep-

ing ω_2 , ω_1 being fixed. One finds that the variations with Δ of the intensity of the fluorescence light emitted by the atom (fluorescence rate R_F) have the shape represented in Fig. 3b: R_F vanishes for $\Delta = 0$ and then increases, forming a narrow dip. The width Γ' of this dip is determined by the relaxation time in the ground state and is much smaller than the width Γ of the excited state.

The interpretation of this effect involves a quantum destructive interference. The atom can absorb a photon ω_1 from g_1 and go to e , with an amplitude Ω_1 , where Ω_1 is the Rabi frequency characterizing the coupling of the atom with laser 1. It can also absorb a photon ω_2 from g_2 and go to e , with an amplitude proportional to Ω_2 . But, if the atom has been put in a linear superposition of g_1 and g_2 :

$$|\psi_D\rangle = c_1|g_1\rangle + c_2|g_2\rangle, \quad (2)$$

such that

$$c_1\Omega_1 + c_2\Omega_2 = 0, \quad (3)$$

then, the two absorption amplitudes $c_1\Omega_1$ and $c_2\Omega_2$ interfere destructively and the absorption of light is quenched. The state $|\psi_D\rangle$ is called for that reason a “dark state.” Atoms are trapped in a coherent superposition of the two lower levels, hence the name “coherent population trapping” (CPT) given to this effect. Coherent population trapping and dark resonances were first observed in Pisa [10] and investigated theoretically using optical Bloch equations [11] or a dressed atom approach [12]. They gave rise to several important applications like “electromagnetically induced transparency” (EIT) [13] or “stimulated Raman adiabatic passage” (STIRAP) [14, 15]. We describe now how these effects have allowed a cooling of helium below the single photon recoil limit.

Up to now, we have implicitly supposed that the atom is at rest. If the atom is moving with a velocity \mathbf{v} , the laser frequencies are shifted by amounts equal to $\mathbf{k}_1 \cdot \mathbf{v}$ and $\mathbf{k}_2 \cdot \mathbf{v}$, respectively. In a Raman stimulated process these two Doppler shifts add with a negative sign. The resonance Raman condition remains ful-

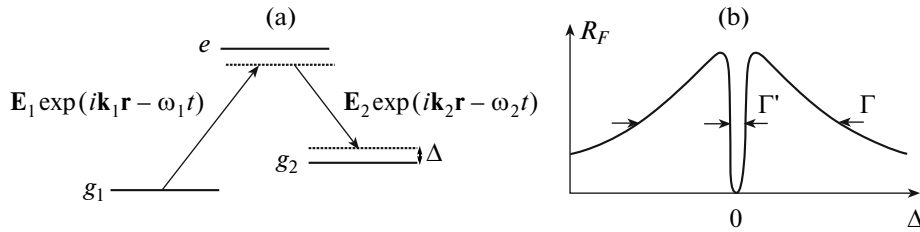


Fig. 3. (a) Three-level atom g_1, g_2, e interacting with two laser waves exciting the 2 transitions $g_1 \rightarrow e$ and $g_2 \rightarrow e$, respectively. (b) Variation of the fluorescence rate R_F with the detuning Δ from the Raman resonance condition.

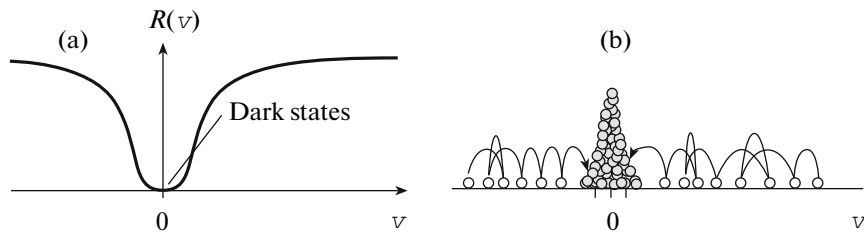


Fig. 4. Principle of laser cooling by velocity selective coherent population trapping (VSCPT). (a) The fluorescence rate $R_f(v)$ vanishes for $v = 0$. (b) The atoms perform a random walk in velocity space and accumulate in the vicinity of $v = 0$.

filled only if the two Doppler shifts are equal. An interesting situation occurs when

$$\mathbf{k}_1 \cdot \mathbf{v} \neq \mathbf{k}_2 \cdot \mathbf{v}. \quad (4)$$

The state which is dark when $\mathbf{v} = \mathbf{0}$ is no longer dark when the atom is moving. An atom at rest cannot absorb light. But, as soon as it is moving, photon absorption processes can take place. Coherent population trapping becomes velocity selective. The absorption rate $R(v)$ is then velocity dependent. It vanishes for $v = 0$ and its variations with v have the shape represented in Fig. 4a. Atoms with zero velocity (or with v very close to $v = 0$) do not absorb light and are protected from the “bad effects” of light, associated with the random recoils due to spontaneous emission processes following the absorption of photons. Atoms with non zero velocity undergo fluorescence cycles. The velocity changes associated with the random recoils due to spontaneous emission can make them falling in the region close to $v = 0$ where they remain trapped and accumulate. This cooling scheme is thus based, not on a friction mechanism, but on a velocity dependent random walk in velocity space with a trap in this space near $v = 0$ where atoms can accumulate. Note that the longer the interaction time θ , the narrower the interval δv around $v = 0$ in which the atoms can remain trapped during θ . One can thus have, after a long enough interaction time, $\delta p = m\delta v < \hbar k$. Contrary to other cooling schemes where fluorescence cycles never stop, VSCPT cooling can be subrecoil.

When $\delta p = m\delta v < \hbar k$, the coherence length of the atomic wave packets becomes larger than the laser wavelength and these wave packets can no longer be considered as localized in the laser waves, so that a quantum treatment of the external atomic degrees of freedom becomes necessary. External quantum numbers, like the atomic momentum \mathbf{p} , must be introduced. Because of the conservation of the total momentum, the three states which are coupled in the stimulated Raman process are g_1 , $\mathbf{p} - \hbar\mathbf{k}_1$, g_2 , $\mathbf{p} - \hbar\mathbf{k}_2$ and e , \mathbf{p} . The dark state is thus a superposition of two states differing, not only by the internal state g_i , but also by the translational state $\mathbf{p} - \hbar\mathbf{k}_i$:

$$|\psi_D\rangle = c_1|g_1, \mathbf{p} - \hbar\mathbf{k}_1\rangle + c_2|g_2, \mathbf{p} - \hbar\mathbf{k}_2\rangle, \quad (5)$$

where \mathbf{p} is such that the Raman resonance condition, including the kinetic energies of the atomic states, is fulfilled:

$$\begin{aligned} E_{g_1} + (\mathbf{p} - \hbar\mathbf{k}_1)^2/2m + \hbar\omega_1 \\ = E_{g_2} + (\mathbf{p} - \hbar\mathbf{k}_2)^2/2m + \hbar\omega_2. \end{aligned} \quad (6)$$

Subrecoil cooling by VSCPT was first proposed and demonstrated in [16]. For detailed calculations, see [17, 18]. Another method for producing a velocity dependent absorption rate $R(v)$ having the shape represented in Fig. 4a has been proposed and demonstrated in [19]. It is not based on dark resonances, but uses sequences of stimulated Raman and optical pumping pulses.

Subrecoil VSCPT cooling has been experimentally demonstrated on helium atoms in the 2^3S_1 metastable state excited by 2 coherent counterpropagating laser beams with the same frequency, close to the frequency of the $2^3S_1 \leftrightarrow 2^3P_1$ transition at 1083 nm, and with σ_+ and σ_- polarizations, respectively (see Fig. 2). If the static magnetic field is equal to 0, the 2 lower states $g_{\pm 1}$ have the same energy. Since the 2 laser frequencies are the same, the Raman resonance condition (6) then gives $p = 0$ and the dark state is:

$$|\psi_D\rangle = \frac{1}{\sqrt{2}}[|M = -1, -\hbar k\rangle + |M = +1, +\hbar k\rangle]. \quad (7)$$

This is an internal-external entangled state with a double peak momentum distribution (see left part of Fig. 5). The fact that two peaks are clearly resolved means that their width δp is smaller than their splitting $2\hbar k$. In fact, the width of the peaks of Fig. 5 is essentially determined by the experimental resolution. A more precise experiment based on a direct measurement of the spatial correlation function of the atoms [20] showed that the momentum width δp was about 30 times smaller than $\hbar k$ (temperatures in the nanokelvin range). By switching off slowly one of the two laser beams, one can transform adiabatically the dark state from a double component state, like (7), into a single component one without any loss of atoms. The physical interpretation of this transformation is analogous to the one given for STIRAP.

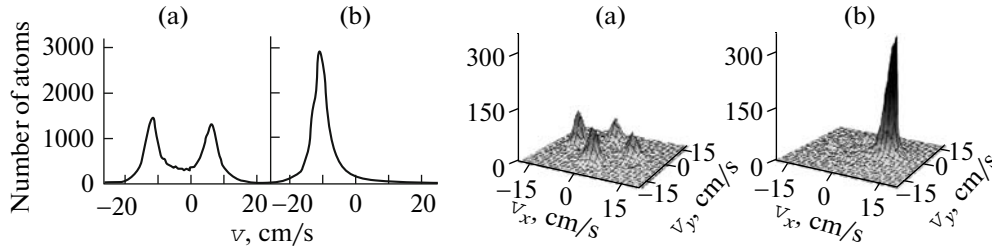


Fig. 5. (Left part) One-dimensional VSCPT cooling experiment performed with two counterpropagating σ_+ and σ_- laser beams. (a) Double peak velocity distribution. The fact that the two peaks, separated by $2\hbar k$, are resolved proves the subrecoil character of the cooling. (b) Single peak observed without any loss of atoms when one of the two laser beams is switched off slowly. (Right part) Two-dimensional VSCPT cooling experiment performed with two orthogonal pairs of counterpropagating σ_+ and σ_- laser beams in the xy plane. (a) Four peak velocity distribution. The four peaks are well resolved. (b) Single peak observed without any loss of atoms when three of the four laser beams are switched off slowly.

These experiments are one-dimensional cooling experiments. It has been shown [21] that, for a $J_g = 1 \leftrightarrow J_e = 1$ transition, like the one studied here, VSCPT cooling can be extended to two and three dimensions. The dark state is then isomorphic to the laser configuration, which means that, if we have four laser beams propagating along the positive and negative directions of two perpendicular axis, the dark state is a linear superposition of four atomic wave packets propagating along the same directions with different internal states. Two and three dimensional VSCPT cooling experiments have been done [22, 23]. When they are combined with STIRAP type adiabatic transfers, they provide the possibility to manipulate three-dimensional wave packets in the nanokelvin range (see right part of Fig. 5).

2.3. How to Get a High Phase Space Density?

VSCPT cooling has no lower limit in temperature. One can show that the width of the velocity distribution decreases indefinitely when the interaction time increases.² But, if the goal of the experiment is to reach the threshold for Bose-Einstein condensation, it is not enough to decrease δp . One must increase the density in phase space. It is unfortunately too difficult to reach high spatial densities with VSCPT. The limitation comes from multiple scattering of light. The photons emitted by the atoms performing the random walk in v -space towards $v = 0$ can be reabsorbed by the atoms already put in the dark state because these photons have not necessarily the good polarization for preventing absorption to occur. The increase of the vapor density is thus limited by this effect.

To overcome this difficulty, the next step is therefore, like in all other BEC experiments, to use evaporative cooling with atoms which have been laser pre-

cooled. The key issue is then to have elastic collision rates much larger than the inelastic collision rates due to Penning ionization. It was not obvious when these experiments started that such a condition will be fulfilled. We describe in the next section experimental results showing that the inhibition of Penning collisions due to the conservation of the total spin was fortunately good enough for allowing the observation of BEC on metastable helium.

3. BOSE-EINSTEIN CONDENSATION OF METASTABLE HELIUM

3.1. Experimental Realization of a Condensate

The final stage of cooling to reach Bose-Einstein condensation is a spatial compression of the cold cloud in a magnetic trap [6]. In our experiment all coils were external to the quartz cell and produced an anisotropic magnetic Ioffe-Pritchard trap, to which a pair of Helmholtz coils were added in order to reduce the bias field and thus to increase the radial confinement. After switching off the MOT field, the sample is first cooled down to about 300 μK in a molasses phase. Then the atoms are optically pumped into a unique Zeeman sublevel in order to maximize the transfer into the magnetic trap, which retains only atoms in the same spin state. The final step of the experiment is evaporative cooling induced by radiofrequency induced spin-flip. Rapid thermal equilibration is necessary for the forced RF evaporation which selectively removes the atoms at the high end of the velocity distribution. A RF ramp lasting about 10 s is necessary to cool the atomic cloud to just a few microkelvins, meanwhile the density climbs up to roughly 10^{13} atoms/cm³.

The appearance of the condensed fraction clearly shows as a narrow structure on the image taken after expansion of the cloud falling in free flight. The signature of the condensation is given by the evolution of the shape of this structure in a time of flight measurement: the ellipticity of the image reverses when the

² There is of course the limitation to δp introduced by the Heisenberg uncertainty relation $\delta p \delta x \geq \hbar$, where δx is the spatial extent of the atomic wave packets limited by the size of the cell containing the atoms.

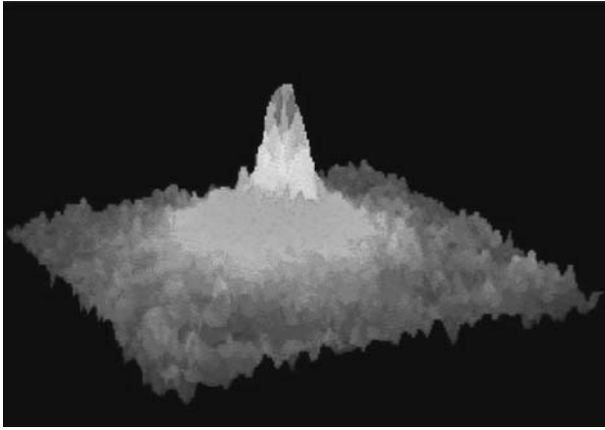


Fig. 6. False color picture of a Bose–Einstein condensate of metastable helium. One clearly sees a narrow peak corresponding to the condensate above a broad pedestal corresponding to the thermal cloud.

expansion time is increased, due to the mean-field interaction between the atoms in the condensate. Also the 1D profile of an absorption image displays a characteristic bimodal structure, with a parabolic shape for the condensed fraction appearing on top of the thermal component. The critical temperature for appearance of the condensation is close to $4 \mu\text{K}$ with the maximum atomic densities we were able to produce. The typical decay time of the condensate is 2 s, due to inelastic collisions between metastable atoms. It was not possible to distinguish between 2-body and 3-body collisions, but the data allowed to place an upper bound on the rate constants for these two decay mechanisms.

3.2. How to Measure the Scattering Length

When we obtained the helium condensation at ENS we were first concerned with the measurement of the scattering length characterizing the interaction between two metastable atoms at low temperature. For this we had to know the number of atoms in the sample. A maximum value of this number was estimated to be of the order of a few 10^5 . However its precise value was found difficult to obtain, due to several experimental sources of error. The method is based on the interpretation of absorption images obtained with a resonant probe beam after the current in the trap coils is turned off. First, remanent eddy currents might shift the atomic frequency with respect to the probe beam frequency, even if a long time delay is imposed between the measurement and the switch-off of the trap current. Second, the laser linewidth broadens the absorption lineshape and reduces the absorption cross-section. Third, the metastable atoms have a huge Penning ionization in the presence of resonance light, so that losses accumulate during the probe pulse at high

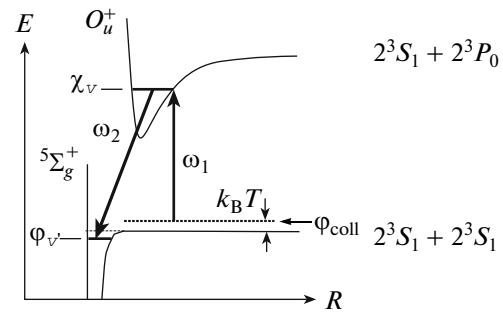


Fig. 7. Principle of one-photon and two-photon photo-association. In a one-photon photo-association experiment, a pair of colliding atoms in the ϕ_{coll} state is excited by a laser with frequency ω_1 in a vibrational state χ_v of an excited molecular potential. If a second laser with frequency ω_2 is added, exciting the transition from χ_v to a vibrational state ϕ_v of the lower molecular potential, the production of molecules in the ϕ_v state is called two-photon photo-association.

intensity; however operating at low intensity is not compatible with sufficient signal to noise ratio. Several corrections were applied to deduce a value for N which could not be determined with an accuracy better than 50%.

On the other hand the chemical potential μ could be extracted from the size of the expanding condensate in time of flight. Using this value of μ and the approximate value of N , one could derive a measurement of the s -wave scattering length a for interacting polarized metastable helium atoms. We found $a = (16 \pm 8) \text{ nm}$, the error being mainly due to the uncertainty on the number of atoms. The group in Orsay, which also obtained condensation in 2001, found a value for a with a similar error bar $a = (20 \pm 10) \text{ nm}$ [7]. Later different values of a were produced by other methods. The Amsterdam group found $a = (10 \pm 5) \text{ nm}$ derived from evaporative cooling rate [24]. The Orsay group used another method based on the observation of inelastic collisions, combined with the measurement of the threshold of the condensation: their new value was more precise than the previous one as they found $a = (11.3_{-1.0}^{+2.5}) \text{ nm}$ [25]. This uncertainty on the determination of a finally induced our group to turn to photoassociation, in order to find a method based on spectroscopy to derive a fully reliable value for this crucial parameter. We performed one-photon and two-photon photoassociation experiments whose principle is sketched in Fig. 7.

4. GIANT DIMMERS PRODUCED BY ONE-PHOTON PHOTOASSOCIATION

4.1. Principle of the Experiment

Obtaining He_2 molecules runs counter to the intuitive expectation, based on the well known fact that

helium is chemically inert and that He_2 should not exist under normal conditions. Nevertheless our group was able to produce dimmers formed when two polarized metastable ^4He atoms, each carrying 20 eV of electronic energy, collectively absorb a laser photon in a photoassociation process (PA) [8]. The laser in this case connects the 2^3S_1 metastable state to the 2^3P_0 excited state. One reaches the 0_u^+ excited molecular potential which is shown in Fig. 7. This potential has quite peculiar features. It results from the combination of the fine-structure coupling and of the dipole-dipole interaction, which varies in $1/r^3$ as a function of the distance r between the particles. For this potential, the atomic dipoles are oriented so as to produce repulsion at distances shorter than $150a_0$ and attraction for distances greater than this. This has two consequences: first the 0_u^+ potential is purely long range, showing a minimum internuclear distance of $150a_0$. Second it is very shallow; the depth of the molecular potential which binds the atoms together is 2 GHz, namely four orders of magnitude smaller than usual in molecular physics.

The excited molecules created in the 0_u^+ potential exhibit an extremely well resolved spectrum of 5 vibrational levels ($v = 0$ to 4) whose lifetime is of the order of a few microseconds. The scheme of the experiment is shown in Fig. 8. The ‘‘calorimetric’’ detection is an original method which is here preferred to the other detection means such as the trap losses. Actually we observed that the temperature of the cloud increases when the photon excites a pair of atoms and forms dimmers. The temperature rise is large, up to 10 μK above the average temperature of the cloud of typically 4 μK . The heating mechanism that produces the signals can be understood as follows: the molecular dimmers decay radiatively into two fast metastable atoms, carrying away a kinetic energy corresponding to the binding energy of the excited molecule in the 0_u^+ potential. Part of these decay products are expelled from the trap, but a small fraction of them is retained. These trapped atoms are ‘‘hot’’ compared to the rest of the sample and they heat up the cloud.

4.2. Vibrational Spectrum in the 0_u^+ Molecular Potential

The absorption of the photoassociation photon occurs at well defined and widely separated frequencies and was measured with a great accuracy. The PA beam was derived from a cavity-stabilized laser of 0.3 MHz linewidth, locked to the $2^3S_1 - 2^3P_0$ transition. The PA beam pulse was applied for a time ranging from 0.1 to 10.0 ms and the laser frequency was scanned down from the asymptotic value of the atomic transition, with an intensity always set below the atomic saturation intensity. The temperature of the

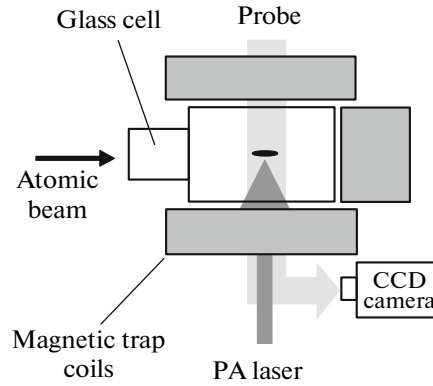


Fig. 8. Scheme of the one-photon photo-association experiment. After a PA laser pulse of a few ms, the trap is turned off and the CCD camera registers an absorption image of the expanding cloud, from which the temperature is deduced.

cloud was monitored at each step. In all, the five bound states were found in the 0_u^+ well. They were fit with a Lorentzian profile and probed under different conditions of magnetic field and density. No dependence of the line center was found. No light shifts were observed either, as the PA beam intensity was kept very low. The temperature was varied from 2 to 30 μK and the line center position extrapolated to zero temperature. Finally a value was found for the binding energy of all 5 vibrational molecular levels in the 0_u^+ potential well.

These experimental energy values were compared to theoretical calculations. We had to calculate the coupling between the atomic orbitals of one atom in the 2^3S_1 state and another in the 2^3P state, the coupling being constructed as a perturbative Hamiltonian in the basis of the fine-structure free states. At large internuclear distances r , the lowest order term of the electromagnetic interaction is the retarded dipole-dipole interaction, determined by the C_3 coefficient. The Hamiltonian including dipole-dipole interaction, fine structure and molecular rotation was diagonalized numerically. The large internuclear distance justified that the next-order term in C_6/r^6 of the electromagnetic interaction was neglected. Measured and calculated binding energies in the 0_u^+ potential agreed very well, to better than 1%.

The agreement is especially remarkable because the calculation model completely neglects the not so well-known electrostatic repulsion providing the inner-wall for normal molecules. Here, the full r -dependence emerges only from the purely long range interactions in $1/r^3$, even for short distances. The distance between the two atoms in the molecule is so large that the retardation in the propagation of the dipole-dipole interaction between them becomes non negligi-

ble and have been included in the theoretical analysis of the spectrum. For instance for the $\nu = 1$ level the contribution of retardation effects is on the order of 1% of the binding energy, whereas the relative experimental uncertainty of the measurement is on the order of 10^{-3} . The comparison of experimental and theoretical data clearly shows a better agreement when retardation effects are taken into account.

4.3. Exotic Character of the Dimmers

We want to stress the very peculiar character of these helium molecules. First they are built from a pair of two excited atoms, which is quite unusual. Second one notes that these dimmers are giant. The separation between the bound pair of atoms is of the order of 50 nm, or nearly one thousand times larger than normal bond lengths. This size, which approaches that of a virus, makes these the most distended two-atom molecules ever observed. The existence of “purely long range” molecules had been predicted long ago by Stwalley and already observed with cesium atoms. However helium is the simplest atom for which such molecular states have been studied and the comparison between experiment and theory is by far the most accurate.

One notes that in these giant dimmers the two initial metastable helium atoms are constantly kept apart from each other by a very large distance, above 10 nm: this is the reason why these molecules exhibit a finite lifetime. This would not be the case if the two atoms in the molecule could approach each other to shorter distances, as with usual dimmers, because the Penning ionization mechanism would destroy the molecule in an extremely short time. The large separation of two metastable helium atoms in a giant dimmer is thus another mechanism, as well as the spin polarization, to inhibit the fast destruction of metastable helium by Penning ionization.

4.4. Measuring the Scattering Length with Light Shifts

The one-photon photoassociation experiments with metastable helium unexpectedly led us to a first precise measurement of the s -wave scattering length a . We observed that when the PA laser beam intensity was increased, light-induced frequency shifts appeared in the spectra. This phenomenon was studied and out of its interpretation a value of a was derived [26]. The shifts arise from the optical coupling of the molecular excited state with the continuum of the scattering states and with the bound states of the two colliding 2^3S_1 atoms. They can be described by a theoretical calculation based on the theory developed by Bohn and Julienne [28].

The dependance of the shift on the parameter a has two origins. One must first consider the energy of the

least bound state in the $5\Sigma_g^+$ interaction potential between the two spin-polarized metastable helium. This state is a vibrational state $\nu = 14$, very close to the dissociation limit and its binding energy $E_{\nu=14}$ varies as $1/a^2$. At ultracold temperature, the atoms collide with a very small relative kinetic energy. When the laser is tuned in the vicinity of the free-bound transition, it is thus not far from resonance with the transition connecting the excited state to the $\nu = 14$ state. Consequently, the light shift of the excited state is appreciably dependent on the energy $E_{\nu=14}$ and thus on a . Second, the optical coupling of the excited state with the bound state and the scattering states above the quintet potential involve Franck-Condon overlaps, which depend critically on a .

The measurements were performed using the calorimetric method described above. The position of the spectral lines was measured as a function of the PA laser intensity and for several vibrational levels of the 0_u^+ potential. The shifts as expected were found to increase linearly with the laser intensity. The ratio between the slopes achieved in same experimental conditions for different ν states were used to compare with theory. In this way the uncertainty on the laser intensity at the cloud location was eliminated. The comparison of the experimental ratios with the calculated ones as a function of parameter a provided a value of a with some error bar resulting from the experimental uncertainties. Different couples of ν states provided compatible values of a . We thus derived the value $a = 7.2 \pm 0.6$ nm, significantly lower than previous results obtained by non-spectroscopic methods.

5. TWO-PHOTON PHOTOASSOCIATION AND ATOM-MOLECULE DARK RESONANCES

5.1. Observation of the Dark Resonance

Two-photon photo-association experiments following the scheme of Fig. 7 have been performed on helium atoms [9]. The state χ_{ν} is the vibrational state $\nu = 0$ of the 0_u^+ potential. The state φ_{ν} is the least vibrational state $\nu = 14$ of the $5\Sigma_g^+$ potential. Dark resonances have been observed in this configuration³ and their shape found in good agreement with the theoretical predictions of reference [28]. Figure 9 shows an example of such a dark resonance. It looks quite similar to the dark resonances observed with atoms (see Fig. 4b). There are however important differences. The state φ_{coll} is not a discrete state but belongs to a continuum, so that the dark resonance should be broad. However, since the atoms are ultracold, their energy spread, on the order of $k_B T$, is very small, and

³ Dark resonances have been also observed by two other groups studying two-photon photo-association of alkali atoms [29, 30].

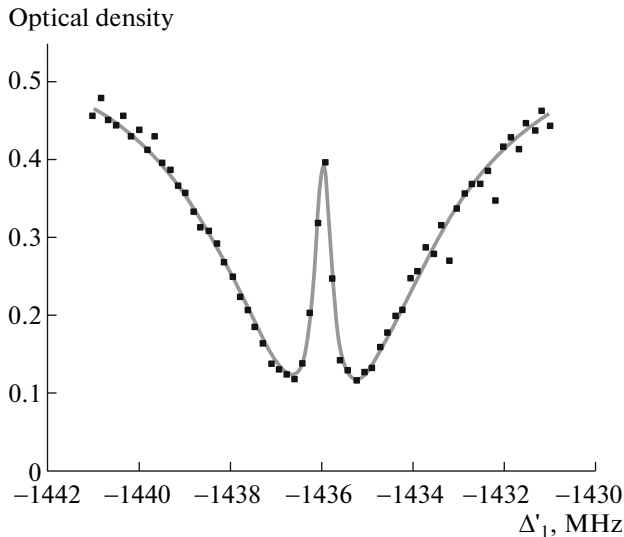


Fig. 9. Example of a dark resonance obtained by scanning the frequency of one of the two lasers.

the corresponding broadening of the dark resonance is generally negligible. Second, the three-level system is not closed: the total population can decrease because of Penning ionization processes. One can show [27] that this prevents the fluorescence rate to vanish completely when the Raman resonance condition is fulfilled. The dark resonance still appears as a dip, but this dip does not go to zero.

5.2. Determination of the Scattering Length

From the position of the dark resonance, one can deduce a very precise value of the binding energy of the least bound state $\nu = 14$ of the $^5\Sigma_g^+$ potential. From this binding energy one can, using good theoretical calculations of the $^5\Sigma_g^+$ potential [31], derive a value of the scattering length a of two helium atoms in the metastable state: $a = 7.512 \pm 0.005$ nm. This value is more than one hundred times more precise than all previous other measurements. From the width of the dark resonance, one can also deduce information on the lifetime of the $\nu = 14$ state and investigate the effect of Penning collisions in a molecular bound state.

6. CONCLUSIONS

This article has recalled several steps of the work done in our group at ENS in the domain of helium physics. Metastable helium atoms, as well as the exotic molecules produced when two such atoms are simultaneously excited, have unique features all related to the large electronic energy carried by the metastable atom. We stressed in particular the general character of the methods based on dark resonances with Λ schemes, showing analogies between sub-recoil cool-

ing of the metastable atoms by VSCPT on one hand, molecule-atom dark resonance with Raman photoassociation on the other hand. This review demonstrated also several ways to inhibit the fast rate of Penning ionization collisions between metastable atoms, one based on the electronic spin polarization, the other one on the imposed minimum distance between two atoms in a giant dimmer.

In the future our group plans to study quantum phase transitions with the metastable helium condensate loaded in an optical lattice. The idea is to exploit the unique property of the metastable atoms which is to Penning ionize when close to each other: the measurement of ion rate production will be the tool to handle the dynamics in real time for processes such as the alteration of the Penning collision rates when the condensate is squeezed in 1D or 2D lattices, or the superfluid—Mott insulator transition in 3D lattice. In the Mott phase all metastable atoms being isolated in distinct sites will have a very low probability to Penning annihilate, and this is a one more method to keep them together for a long time and store the total of the internal energy that they individually carry.

REFERENCES

1. F. D. Colegrove, L. D. Shearer and G. K. Walters, *Phys. Rev.* **132**, 2561 (1963)
2. D. S. Betts and M. Leduc, *Ann. Phys. Fr.* **11**, 267 (1986)
3. C. Lhuillier and F. Laloe, *J. de Phys.* **40**, 239 (1979).
4. P. J. Nacher, G. Tastevin, M. Leduc, S. B. Crampton, and F. Laloe, *J. Phys. Lett.* **45**, 441 (1984).
5. P. O. Fedichev, M. W. Reynolds, U. M. Rahmanov, and G. V. Shlyapnikov, *Phys. Rev. A* **53**, 1447 (1996).
6. F. Pereira Dos Santos, J. Léonard, J. Wang, C. J. Barrelet, F. Perales, E. Rasel, C. S. Unnikrishnan, M. Leduc, and C. Cohen-Tannoudji, *Phys. Rev. Lett.* **86**, 3459 (2001).
7. A. Robert, O. Sirjean, A. Browaeys, J. Poupard, S. Nowak, D. Boiron, C. I. Westbrook, and A. Aspect, *Sci. Magazine* **292**, 463 (2001).
8. J. Léonard, M. Walhout, A. P. Mosk, T. Muller, M. Leduc, and C. Cohen-Tannoudji, *Phys. Rev. Lett.* **91**, 073203 (2003).
9. S. Moal, M. Portier, J. Kim, J. Dugué, U. D. Rapol, M. Leduc, and C. Cohen-Tannoudji, *Phys. Rev. Lett.* **96**, 023203 (2006).
10. G. Alzetta, A. Gozzini, L. Moi, and G. Orriols, *Nuovo Cim. B* **36**, 5 (1976).
11. E. Arimondo and G. Orriols, *Lett. Nuovo Cim.* **17**, 333 (1976).
12. J. Dalibard, S. Reynaud, and C. Cohen-Tannoudji, in *Interaction of Radiation with Matter*, Volume in honour of A. Gozzini, Ed. by L. Radicati (Pise, 1987), p. 29.
13. S. E. Harris, *Phys. Today*, No. 6, 36 (1997).
14. J. R. Kulinski, U. Gaubatz, F. T. Hioe and K. Bergmann, *Phys. Rev. A* **40**, 6741 (1989).

15. N. V. Vitanov, M. Fleischauer, B. W. Shore, and K. Bergmann, *Adv. At. Mol. Opt. Phys.* **46**, 55 (2001).
16. A. Aspect, E. Arimondo, R. Kaiser, N. Vansteenkiste, and C. Cohen-Tannoudji, *Phys. Rev. Lett.* **61**, 826 (1988).
17. A. Aspect, E. Arimondo, R. Kaiser, N. Vansteenkiste, and C. Cohen-Tannoudji, *J. Opt. Soc. Am. B* **6**, 2112 (1989).
18. C. Cohen-Tannoudji, "Atomic Motion in Laser Light," in *Fundamental Systems in Quantum Optics*, Ed. by J. Dalibard, J.-M. Raimond, and J. Zinn-Justin, Les Houches session LIII 1990 (North-Holland, Amsterdam, 1992), p. 1.
19. M. Kasevich and S. Chu, *Phys. Rev. Lett.* **69**, 1741 (1992).
20. B. Saubamea, T. W. Hijmans, S. Kulin, E. Rasel, E. Peik, M. Leduc, and C. Cohen-Tannoudji, *Phys. Rev. Lett.* **79**, 3146 (1997).
21. M. A. Ol'shany and V. G. Minogin, *Opt. Commun.* **89**, 393 (1992).
22. J. Lawall, F. Bardou, B. Saubamea, K. Shimizu, M. Leduc, A. Aspect, and C. Cohen-Tannoudji, *Phys. Rev. Lett.* **73**, 1915 (1994).
23. J. Lawall, S. Kulin, B. Saubamea, N. Bigelow, M. Leduc, and C. Cohen-Tannoudji, *Phys. Rev. Lett.* **75**, 4194 (1995).
24. R. J. W. Stas, J. M. McNamara, W. Hogervorst, and W. Vassen, *Phys. Rev. Lett.* **93**, 053001 (2004).
25. S. Seidelin, J. V. Gomes, R. Hoppeler, O. Sirjean, D. Boiron, A. Aspect, and C. I. Westbrook, *Phys. Rev. Lett.* **93**, 090409 (2004).
26. J. Kim, S. Moal, M. Portier, J. Dugué, M. Leduc, and C. Cohen-Tannoudji, *Europhys. Lett.* **72**, 548 (2005).
27. M. Portier, PhD Thesis (Univ. of Paris VI, 2007).
28. J. L. Bohn and P. S. Julienne, *Phys. Rev. A* **60**, 414 (1999).
29. P. Dumke, J. D. Weinstein, M. Johanning, K. M. Jones, and P. D. Lett, *Phys. Rev. A* **72**, 041801(R) (2005).
30. K. Winkler, G. Thalhammer, M. Theis, H. Ritsch, R. Grimm, and J. H. Denschlag, *Phys. Rev. Lett.* **95**, 063202 (2005).
31. M. Prybytek and B. Jeziorski, *J. Chem. Phys.* **123**, 134315 (2005).